Gas Turbine Environment Effect on Morphology and Mechanical Properties of Pultruded Composite

Kunigal Shivakumar,[1] Huanchun Chen,[1] Gary Holloway[2]

[1]*Center for Composite Materials Research, Mechanical and Chemical Engineering Department, North Carolina A & T State University, Greensboro, North Carolina 27411*
[2]*Diversitech Inc., 110 Boggs Lane, Suite 230, Cincinnati, Ohio 45246*

Received 12 July 2007; accepted 22 August 2007
DOI 10.1002/app.27551
Published online 27 December 2007 in Wiley InterScience (www.interscience.wiley.com).

ABSTRACT: The effect of gas turbine lubricant oil soaking, thermal cycling and their combination on morphology and tension and flexure properties of pultruded composite was studied. Two types of lubricant oils were used: Mil-L-7808 and Mil-L-23699. Composite samples were oil soaked for 720 h and microscopic analysis and mechanical tests were conducted. Samples were thermal cycled for 600 cycles (RT to 315°C) and measured tension and flexure properties. Samples were oil soaked, thermal cycled and then tested. Results of these three groups of environmentally aged samples were compared with non-aged samples. The significance of aging effect is discussed in the article. © 2007 Wiley Periodicals, Inc. J Appl Polym Sci 108: 189–198, 2008

Key words: composites; mechanical properties; morphology; environmental aging; thermal cycling

INTRODUCTION

Gas turbine environment consists of lubricant oil, thermal cycling and their combination. Aging and degradation of composite materials used in this environment need to be understood to assess their durability and life. The component of interest is engine brush seal, whose bristles are made up of T650 carbon fiber and PT-30 cyanate ester resin pultruded rods.[1] The effect of lubricant oil aging, thermal cycling, and their combination on the pultruded composite is studied and the results are discussed in the present article.

Extensive studies[2–17] have been conducted on oil soaking and thermal cycling effects on uni- and multi-directional polymer composite laminates. Test results showed that oil soaking had no degradation effect on mechanical properties of polymer composites.[2,3] Isothermal aging has caused weight loss, T_g reduction and loss of flexural strength and modulus.[4–6] Microcracking[7–9] and fiber/matrix debonding[10] are the most common failure modes observed in composite laminates subjected to thermal cycling. Thermal cycling has also caused weight loss[9,11,12] and degradation of tensile, compressive, shear and flexural strengths as well as modulus.[13–15] The deterioration in mechanical properties was attributed to a combination of thermal stresses induced by the difference in coefficient of thermal expansion (CTE) and thermal oxidation when the composite is exposed to an oxidative atmosphere. Few researchers[16,17] reported increased tensile strength and modulus, which they attributed to stress relief due to internal cracking. The composites considered heretofore were laminates. No research work has been reported on pultruded composite rods and/or Primaset PT-30 cyanate ester composites.

The objective of this article is to evaluate the effect of environmental conditioning including lubricant oil soaking and thermal cycling on mechanical properties of T650 carbon fiber/Lonza Primaset PT-30 cyanate ester composite rods manufactured by pultrusion process. Experimental plan, experiments, results and discussion are given in the following sections.

EXPERIMENTAL

Materials

The materials considered are Cytec T650 carbon fiber (3k tow) and Primaset PT-30 cyanate ester supplied by Lonza Corporation (Basel, Switzerland). Figure 1 shows the molecular structure of PT-30 cyanate ester. It is a thermoset resin that has 65% char yield (same as phenolics) and less than 0.5% volatiles and generates no gaseous by-products during cure. PT-30 has a low viscosity (80 c.p.s.) at its processing temperature (120°C) and is post-curable to achieve T_g in

Correspondence to: K. Shivakumar (kunigal@ncat.edu).
Contract grant sponsor: US Air Force; contract grant number: 10-JE0507.
Contract grant sponsor: Office of Naval Research; contract grant number: N00014-07-1-0465.

Journal of Applied Polymer Science, Vol. 108, 189–198 (2008)

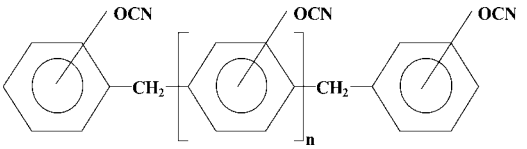

Figure 1 Molecular structure of Primaset PT-30 cyanate ester resin.

excess of 371°C. It has excellent electrical and dielectrical properties and thermo-mechanical stabilities.[18]

Pultrusion process

Pultrusion is a highly automated process for manufacturing composite material parts of constant cross-section shaped profiles. The pultrusion process consists of guiding the T650 fiber tow from a creel through a set of guides, and then pulling through a PT-30 resin bath that is maintained at proper temperature so that the tow is adequately impregnated with the resin. The impregnated fiber tow is then pulled through a hot die, where the tow is shaped into a circular shape. Finally the rod is pulled through a thermal curing chamber to complete the cure. Curing is done in two stages, first at 260°C for 2 min and then at 315°C for another 2 min. The fully cured fiber rod is collected by the take up spool. Using the above process, Aztex (Waltham, MA) produced the rods of diameter 0.5 mm ± 0.01 mm and supplied in lengths of 30 cm. Optical microscopic image and fiber count analysis showed that the fiber volume fraction of the pultruded rod is about 65% ± 1%.

Environmental conditioning

The environmental conditioning involves soaking in lubricant oils for 720 h and thermal cycling. Groups of composite rods were exposed to the following environmental conditions and then were mechanically tested.

a. Base line: As-received samples from the pultruder.
b. Soaking in lubricant oils: The composite rods were soaked in Mil-L-7808 and Mil-L-23699 lubricant oils for a period of 720 h.
c. Thermal cycling without lubricant oil soaking: The rods were thermal cycled for 600 cycles.
d. Thermal cycling with lubricant oil soaking: After soaked in Mil-L-7808 and in Mil-L-23699 for 720 h, the rod specimens were taken out and then thermal cycled for 600 cycles.

Note that the Cases b and d each consist of two groups with two types of lubricants.

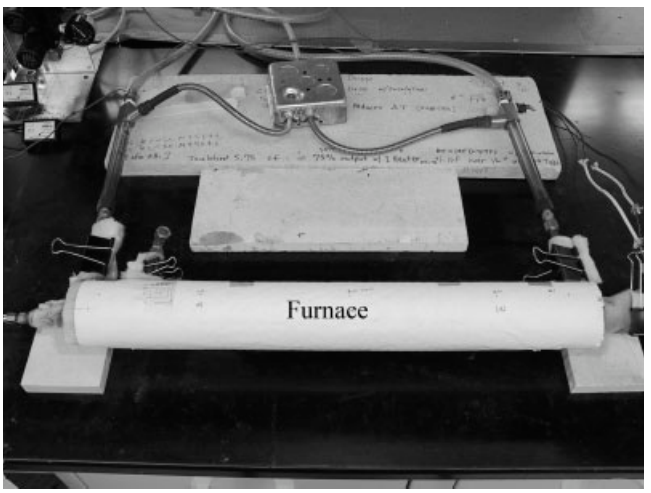

Figure 2 Thermal cycling apparatus.

Conditioning in lubricant oils

The composite rods (a minimum of 20 per grade of oil) were fully immersed in two separate sealed stainless steel containers, one containing Mil-L-7808 and the other containing Mil-L-23699 turbine oil. The rods were then left to soak for 720 h (30 days) in the containers. After the soaking period, the composite rods were drained and wiped free of oil using acetone before proceeding to further conditioning and/or testing.

Thermal cycling

The composite rods were thermally cycled 600 times in a compressed air heating/cooling apparatus specially designed and built for this test (See Fig. 2). Figure 3 shows the proposed and measured temperature profiles for each cycle. Broken lines represent the proposed thermal cycle while the solid lines represent the actual one. The actual cycle almost duplicated the proposed cycle. The only difference is that the heating and cooling ramps were 4 min instead of 2 min. Each thermal cycle contains first holding at RT for 12 min, heat-up from RT to 315°C in 4 min, holding at 315°C for 28 min, cool-down from 315°C

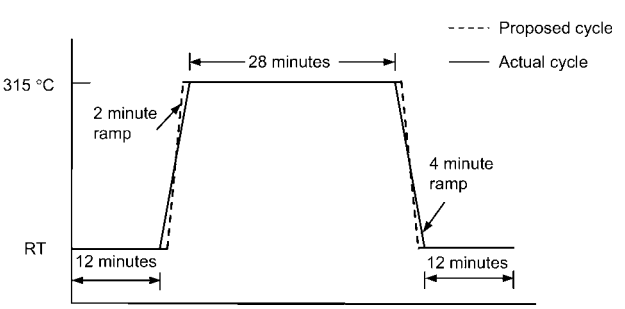

Figure 3 Proposed and actual thermal cycles.

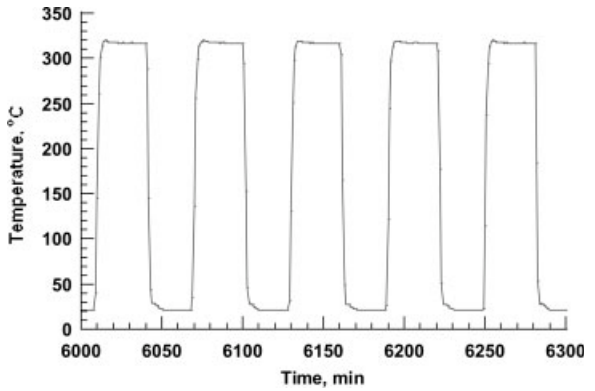

Figure 4 Typical segment from a thermal cycling run.

to RT in 4 min and finally holding at RT for another 12 min. The heating and cooling rate achieved was 73°C/min. Figure 4 shows the typical segment of the temperature profiles acquired during one of the tests. The repeated cyclic data shows the repeativeness of the furnace.

Glass transition temperature (T_g)

Dynamic mechanical analysis (DMA) was performed using DMA 7e from Perkin Elmer to measure the glass transition temperature (T_g) of baseline, oil soaked and 600 thermal cycled composite rods. The specimen configuration was simply-supported beam with a central loading. The specimen span was 20 mm and the central load applied was about 150 mN. Temperature scan test was conducted at 5°C/min with the frequency of 1 Hz. Storage modulus, loss modulus and damping factor (Tanδ) were measured continuously with temperature.

Microscopy of pultruded composite rods

Microscopy analysis was conducted on baseline (as-received), lubricant oil soaked, thermal cycled, and lubricant oil soaked + thermal cycled rod samples. Optical microscope and scanning electron microscope (SEM) images of rod cross-sections were captured and examined to investigate the environmental conditioning effect on the morphologies.

Mechanical testing of pultruded composite rods

Two types of mechanical tests were conducted: tension test to measure ultimate tensile strength, fracture strain and modulus; and three-point bend flexure test to measure flexural modulus and strength.

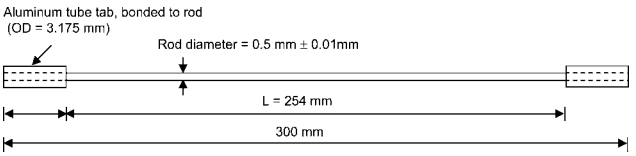

Figure 5 Tension specimen configuration.

Tension test

The tension test specimen configuration is shown in Figure 5. The total length of the specimen was 300 mm and the tab length was 25.4 mm. The composite rod diameter was 0.5 mm with ± 0.01 mm variation. The test-length L, which was 254 mm, was measured to the nearest 0.025 mm for each specimen. Because of the small size of the rod, a special tabbing system was devised and tests were conducted with special instrumentation and procedures.

The ends of the composite rods were immersed into acetone and washed for no less than 5 min for good adhesive bonding. Scotch-Weld Epoxy Adhesive DP-460 was used for bonding. For the collet type gripping technique, 3.175 mm OD aluminum tube segments, cut to 25 mm length, were filled with the adhesive using a syringe. Small rubber O-rings were fitted into the ends with the rod placed through the tube and left overnight to cure at room temperature. Figure 6(a) shows details of the aluminum tube, adhesive, O-rings, and composite rod assembly at the tabbing location. A photograph of the tabbing assembly at one end of a test sample is shown in Figure 6(b).

Each specimen was gripped by double-angle collet grips over the aluminum tube tabs on each end of

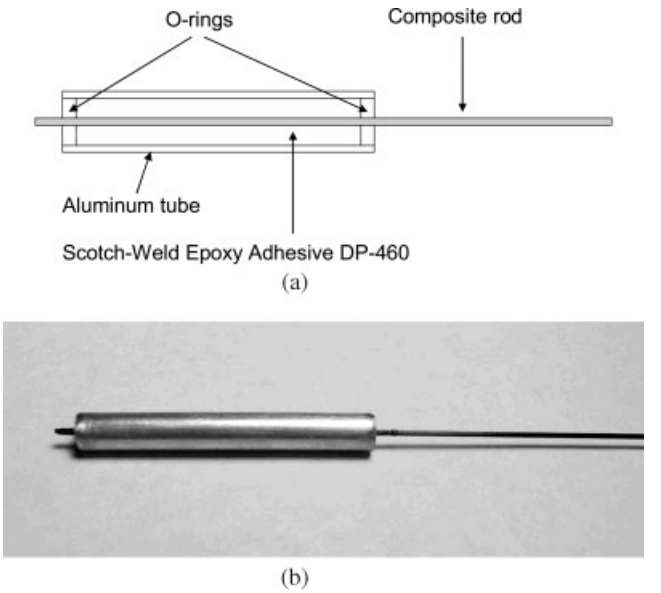

Figure 6 Tabbing and test specimens. (a) schematic of the tabbing; (b) photograph of tab.

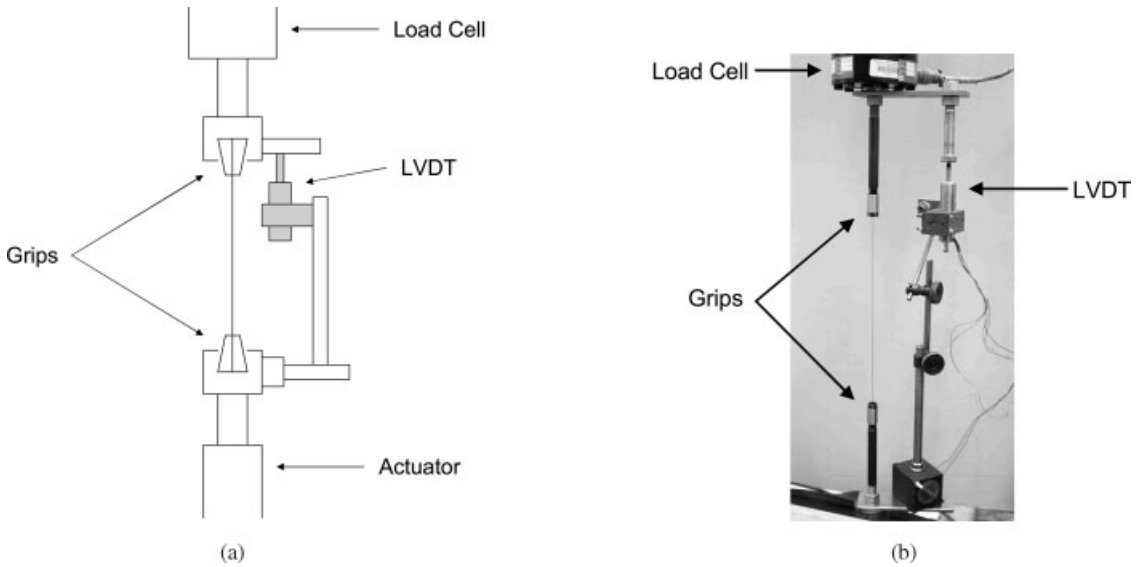

Figure 7 Tension test setup. (a) schematic; (b) photo.

the sample. The collets were tightened with a wrench while load was kept at zero. The grip extensions had been threaded to adapt to the load cell and actuator of MTS 810 testing machine and the load-train re-aligned with the new fixturing installed.

After preliminary testing on dummy specimens, a load cell with a full-scale range of 890 N was chosen for the tests. Load was recorded to the nearest 0.04 N. An LVDT was used to directly measure the change in displacement between the two grips, thus eliminating the load-train deformation if the actuator displacement had been used. Figure 7 shows the schematic (a) and photograph (b) of the instrumentation and test setup of the tension test. The tests were run at a constant displacement rate of 0.5 mm/min. The LVDT displacement reading and the load were recorded continuously (every 0.5 s) during the test. The load and displacement at fracture were recorded and then the tensile strength and fracture strain were calculated.

Flexure test

The purpose of this test is to evaluate the extent of matrix damage because of environmental exposure of the composite rods. The matrix damage due to microcracking and interfacial separation should effect the flexural modulus/stiffness much more readily than the tensile modulus. Therefore a three-point bend test, with a span to diameter ratio of 30 (similar to ASTM Standard D2344), was chosen. The test setup and the specimen are shown in Figure 8. The lower loading supports were 3.175 mm diameter and the upper support was 6.35 mm diameter. Load data was acquired with a resolution of 0.004 ± 0.002 N. The displacement rate was 0.5 mm/min.

For each sample category, three of the 30 cm rods were used for the flexure tests. From each of these

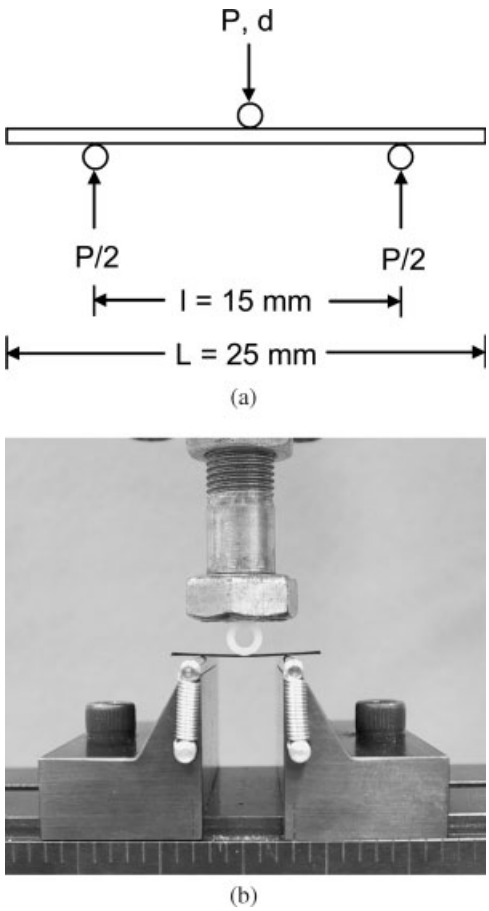

Figure 8 Flexure test setup. (a) schematic; (b) setup.

three rods, the flexure samples were cut as three 25.4 mm segments from one end of the rod. The samples were designated as the first, second, and third inch segments from the ends of the rods. Totally nine specimens were tested for each conditioning case.

RESULTS AND DISCUSSION

Glass transition temperature (T_g)

Using the storage modulus data, T_g was calculated as per ASTM standard E 1640-04. The T_g of four baseline samples ranged from 396 to 416°C with an average of 408°C (same as PT-30 data). Oil soaked rods show a T_g of 412°C, which indicates that oil soaking did not alter the T_g of the composite rods. The 600 thermal cycles increased the T_g to 468°C, demonstrating the fact that the heat treatment does increase the T_g, as evidenced in many thermoset polymer composites.

Microscopy results

Baseline (as-received) composite rods

Figure 9 shows the optical and SEM images of the baseline rod cross-section. Figure 9(a) displays the whole rod cross-section and Figure 9(b) shows the details of fiber distribution. Fibers are uniformly and densely distributed and are well bonded to the resin except at some dark regions indicating voids or resin deficiency. This is verified by the SEM image [See Fig. 9(c)], which shows the details of the resin deficiency. The microscopy examination was repeated at five cross-sections of each rod and for five rods. All the images showed the same trend.

Lubricant oil soaked composite rods

Optical microscopic images of composite rods soaked in Mil-L-7808 and in Mil-L-23699 showed no noticeable morphological change compared with images of as-received rod. This indicates that oil soaking did not affect the morphology of pultruded rod.

Thermal cycled composite rods

Figure 10 shows the morphology of thermal cycled rod cross-section. Widespread microcracking, fiber-matrix debonding/seperation, and matrix shrinkage are seen in these images. The morphology change of the composite rods is the result of combined effects of thermal stress and possible matrix degradation/oxidation. Under the thermal cycling condition, the CTE mismatch between fiber and matrix results in thermal stress at the fiber/matrix interface. This repeated thermal stress cycle could initiate fiber/matrix debonding. Another reason for the debonding could be the degradation of the coupling agent applied on the carbon fibers. The T650 carbon fibers used were sized by an epoxy/urethane sizing agent

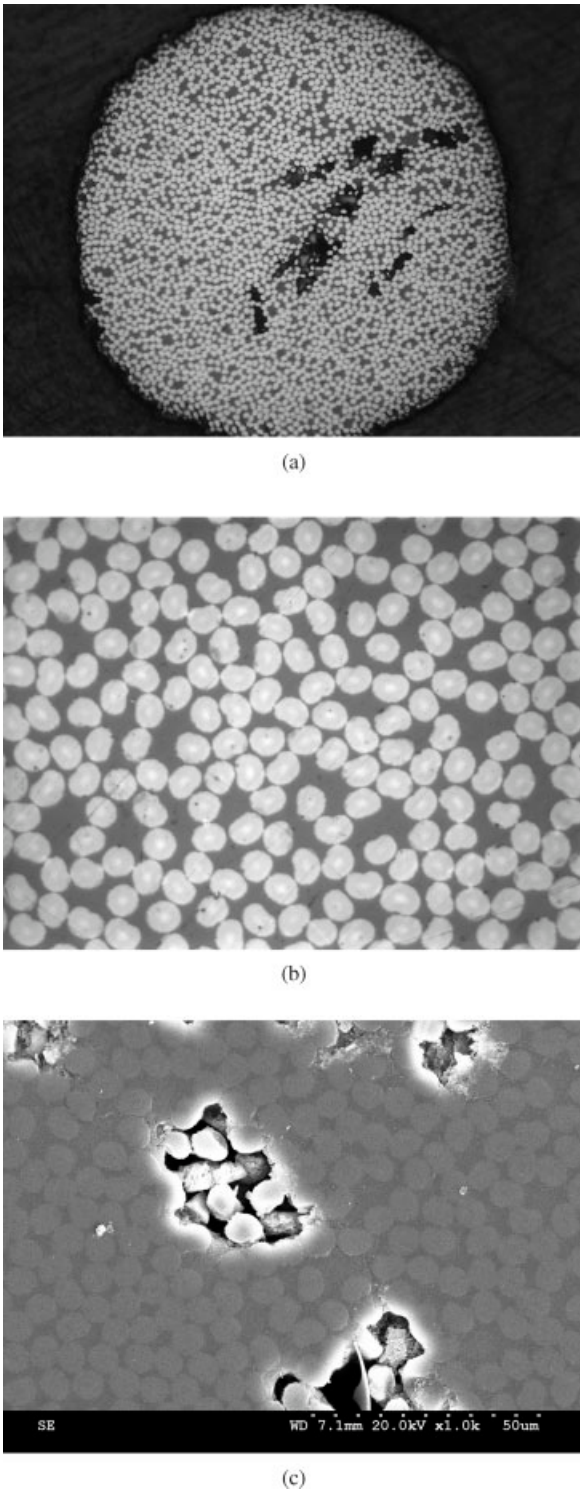

Figure 9 Optical and SEM images of baseline rod cross-section (a) whole rod cross-section (×200); (b) magnification ×1k; (c) details of defective areas (×1k).

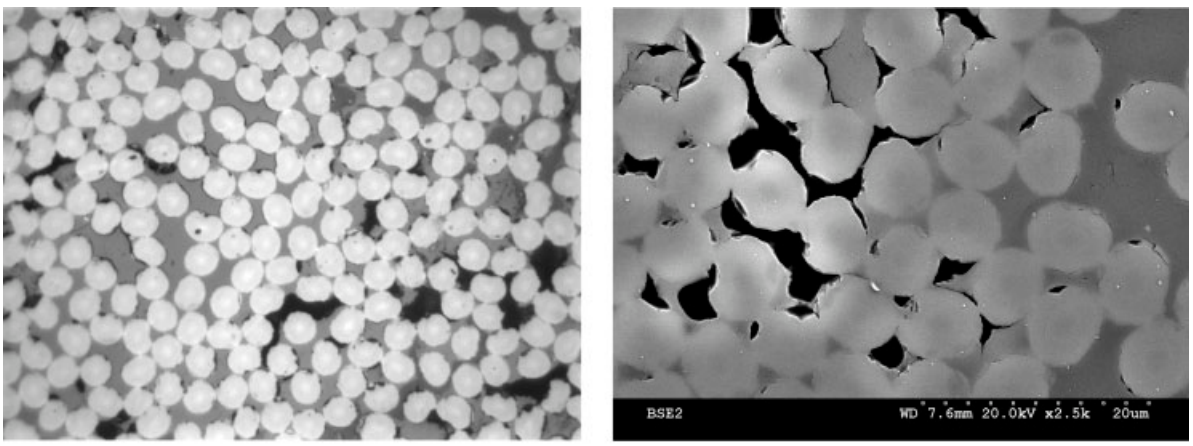

Figure 10 Optical and SEM images of thermal cycled rod cross-section. (a) optical image (×1k); (b) SEM image (×5k).

UC309. This sizing agent starts to decompose at around 210°C and continues to decompose until 400°C. Under the current thermal cycling condition (RT-315°C), the sizing agent decomposes and thus causes fiber/matrix separation. Furthermore, high temperature 315°C in air could have also oxidized the active interface region. The combined effects of these phenomena are seen in the microscopic images.

Lubricant oil soaked + thermal cycled composite rods

Figure 11 shows the SEM image of Mil-L-7808 soaked + thermal cycled rod cross-section. All the lubricant oil soaked + thermal cycled images demonstrated morphologies similar to those of thermal cycled only samples. Therefore, fiber-matrix interfacial separation and matrix cracks are due to thermal cycling effects while lubricant oil soaking has no effect.

Tension test results

For each test specimen, the complete stress-strain response from zero load until failure was acquired. This data gave us strength, modulus, and fracture strain of the test specimen. The stress-strain response for all specimens was found to be linear until the fracture.

The tension test results for baseline, lubricant oil soaked, thermal cycled and lubricant oil soaked + thermal cycled rods are summarized in Table I. The average (average of five tests) values of tensile strength, modulus and fracture strain for each case, percent CV (coefficient of variation) and the percent change in properties compared to the baseline sample are listed. The percent CV is reasonable for all conditions. The modulus of the composite rod is about 138 GPa. The change of modulus due to oil soaking is within 10%. The baseline tensile strength of the composite rods is 1.76 GPa and the fracture strain is 1.27%. Soaking the specimens in the two lubricant oils did not alter the tensile strength and the fracture strain. Thermal cycling for 600 cycles did reduce the tensile strength by 27% and the fracture strain by 28% while the modulus remained unaffected.

For the test specimens that were lubricant oil soaked prior to thermal cycling, the properties closely matched those of the test specimens which were only thermal cycled. The lubricant oil soaking had little effect on the tensile properties either before or after thermal cycling.

Post-test photos in Figures 12–14 illustrate typical tensile failures for baseline, lubricant oil soaked, thermal cycled, and lubricant oil soaked + thermal cycled

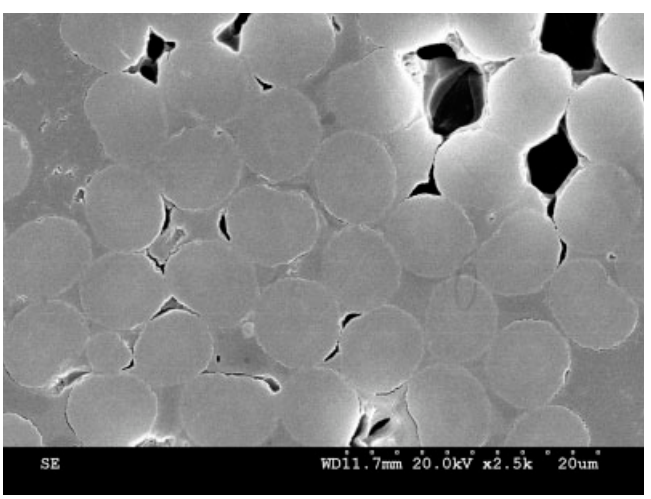

Figure 11 SEM image of Mil-L-7808 soaked + thermal cycled rod cross-section.

TABLE I
Summary of Tension Test Results

Test samples	Tensile strength		Tensile modulus		Fracture strain	
	Strength (GPa)	% Change	Modulus (GPa)	% Change	Strain (%)	% Change
Baseline	1.76 (4.1)*	0	138 (0.9)	0	1.27 (3.8)	0
Mil-L-7808 soaked	1.63 (7.7)	−7	136 (1.8)	−1	1.19 (5.9)	−6
Mil-L-23699 soaked	1.73 (6.3)	−2	139 (1.2)	+1	1.24 (5.6)	−2
Thermal cycled	1.29 (6.5)	−27	144 (0.8)	+5	0.91 (6.7)	−28
Mil-L-7808 Soaked + TC	1.28 (6.3)	−27	137 (4.1)	−1	0.96 (4.9)	−24
Mil-L-23699 soaked + TC	1.19 (6.7)	−32	133 (3.0)	−4	0.91 (7.8)	−28

* Percent coefficient of variation.

test samples. Both baseline and oil-soaked test samples showed brittle fracture typical of unidirectional carbon composite specimens [Fig. 12(a,b)] with the exception of two oil-soaked test specimens [Fig. 12(c,d)]. These two exceptions exhibited splintering, brooming, and finally balling due to high energy release at fracture. These two test samples also had higher strength compared to the oil-soaked samples exhibiting typical brittle failures.

All thermal cycled test specimens, without lubricant oil soaking or with lubricant oil soaking, showed splintering (shattering) of fibers because of degraded matrix properties. These failure modes are illustrated in Figures 13 and 14, respectively.

Flexure test results

Each flexure test determined both the maximum load and the stiffness of the test specimen. The stiffness change from the specimens that are unconditioned to conditioned measured the effect of environmental exposure. The stiffness is defined as the slope of the load- displacement plot, $K_b = \Delta P/\Delta d$, as illustrated in Figure 15(a). Figure 15 shows typical flexure test results for baseline, lubricant oil soaked, thermal cycled and lubricant oil soaked + thermal cycled specimens. Note the different characteristics between the test results for the non thermal cycled and thermal cycled specimens. These differences are explained in Figures 15 and 16.

Figure 16 illustrates a lubricant oil soaked test specimen going through the failure progression. Similar failure progression was seen in all baseline and lubricant oil soaked flexure specimens. Notice the fibers on the underside failing in tension in the last two images as the specimen is deflected at 0.5 mm/min. The load drops each time a group of fibers fails. After stopping the test and unloading the specimen, the specimen becomes straight because of the remaining unbroken fibers at the top.

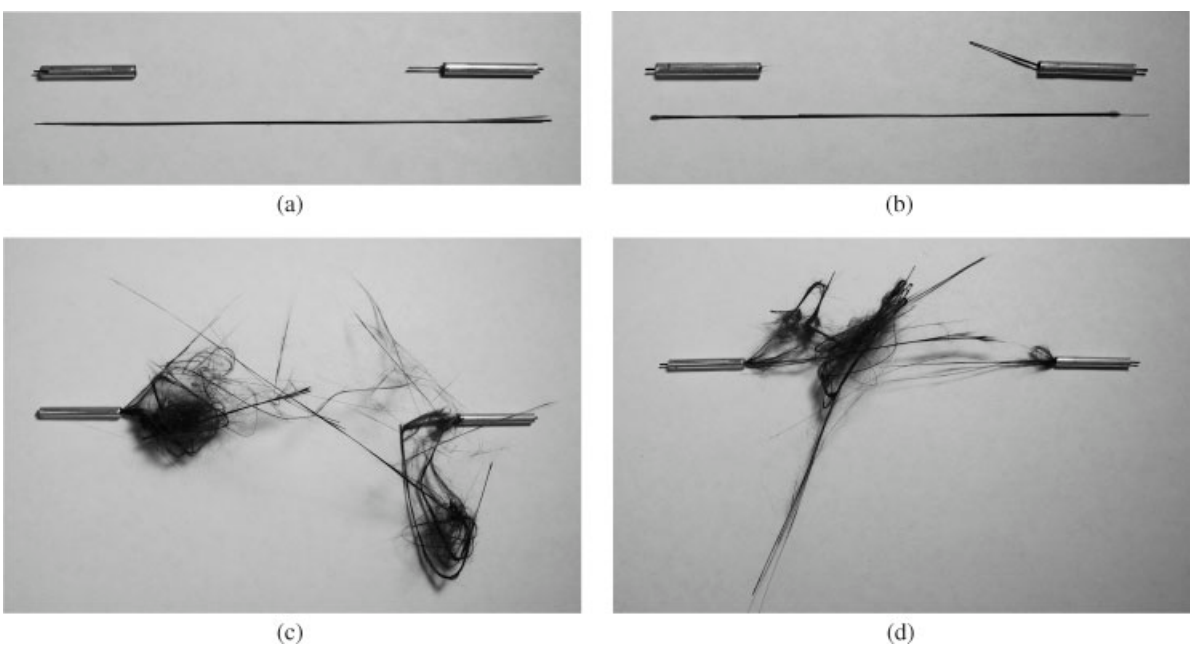

Figure 12 Typical tensile failure modes of baseline and oil soaked composite rods. (a) baseline sample; (b) oil soaked sample #1; (c) oil soaked sample #2; (d) oil soaked sample #3.

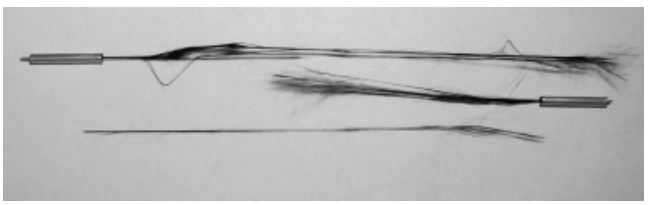

Figure 13 Typical tensile failure modes of thermal cycled composite rods.

Figure 14 Typical tensile failure modes of oil soaked + thermal cycled composite rods.

The flexure specimens of thermal cycled and oil soaked + thermal cycled did not fail as in Figure 16; the load did not drop off suddenly after the initial linear portion of the load-displacement curve and no fibers were seen breaking at the tensile side of the specimen. Instead, the shape of the rod changed

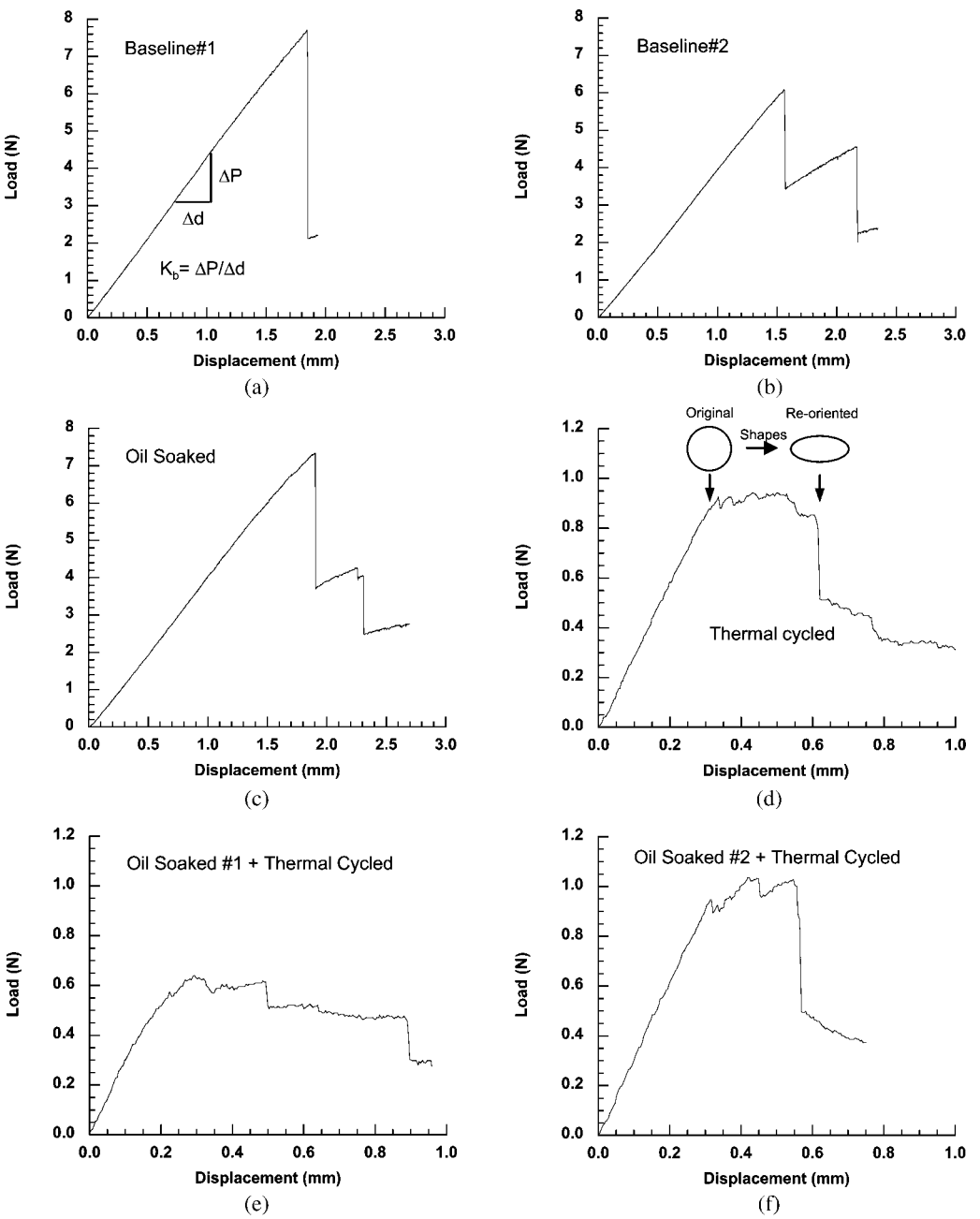

Figure 15 Typical flexure test plots. (a) baseline sample #1; (b) baseline sample #2; (c) oil soaked sample; (d) thermal cycled sample; (e) oil soaked #1 + thermal cycled sample; (f) oil soaked #2 + thermal cycled sample.

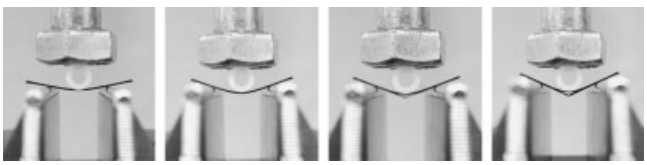

Figure 16 Illustration of failure progression of lubricant oil soaked specimen.

from circular to elliptical as shown in Figure 15(d). During failure, the individual fibers in these specimens re-oriented themselves into an elliptical shape and continued to lose stiffness. The reorientation of fibers is caused by the fiber-matrix interfacial separation and matrix damage as shown previously through the microscopic images (See Fig. 10). Therefore at the middle of the specimen the circular cross-section becomes elliptical as the failure occurs [Fig. 15(d)].

Flexural modulus E_b is calculated from the stiffness K_b using eq. (1), based on the mechanics of materials analysis:

$$E_b = \frac{4l^3 K_b}{3\pi D^4} \quad (1)$$

Where l is the span of three-point bend test, D is the rod diameter and K_b is the flexural stiffness as defined in Figure 15(a). The flexure test results for baseline, lubricant oil soaked, thermal cycled and lubricant oil soaked + thermal cycled rods are summarized in Table II. The average values of maximum or fracture load, flexural modulus and stiffness for each case, percent coefficient of variation (within the parenthesis) and the property change in percentage compared to the baseline specimens are listed. Neither the failure load nor the modulus/stiffness was affected by soaking the specimens in either lubricant. Thermal cycling for 600 cycles, however, did significantly reduce the failure load (by 82%) and the modulus (by 27%). Specimens that were oil soaked in Mil-L-7808 prior to thermal cycling lost 30% of modulus and 87% of failure load whereas the Mil-L-23699 soaking + thermal cycling lowered the modulus by 19% and failure load by 76%.

CONCLUSIONS

This article evaluated the effect of environmental conditioning on tensile and flexural properties of Cytec T650 carbon fiber/Lonza Primaset PT-30 cyanate ester composite rods manufactured by the pultrusion process. The five types of environmental conditioning were as follows: (1) soaking the rods in Mil-L-7808 lubricant oil for 720 h; (2) soaking the rods in Mil-L-23699 lubricant oil for 720 h; (3) thermal cycling the rods for 600 cycles; (4) soaking the rods in Mil-L-7808 oil for 720 h and then thermal cycling the rods for 600 cycles; and (5) soaking the rods in Mil-L-23699 oil for 720 h and then thermal cycling the rods for 600 cycles. Results were compared with as supplied samples. A special high-rate heating/cooling furnace was built, verified, and then used for thermal cycling samples. The heating and cooling rate achieved was about 73°C/min. A special tabbing and tensile gripping method was developed and used. Tensile strength, modulus, and fracture strain were determined and failure modes were recorded. Three-point bend flexure tests were conducted to measure flexural modulus/stiffness, failure load, and failure modes.

The tensile strength of T650/PT-30 pultruded rod was 1.76 GPa with 4% coefficient of variation (CV). The soaking of pultruded rod in the two lubricant oils had little effect on tensile and flexural properties. Microscopic images showed that the oil soaking did not affect the morphology.

Thermal cycling the samples at RT to 315°C for 600 cycles reduced the tensile strength by 27% and the fracture strain by 28%. However, the tensile modulus remained unchanged. Thermal cycling also caused a large reduction in flexural modulus (27%). This was due to reorientation of fibers caused by interfacial separation because of fiber-matrix degradation under thermal cycling condition. For the samples that were oil soaked prior to thermal cycling, the tensile and flexural properties closely matched those of the samples which were only thermal cycled. Microscopy study showed that thermal cycling caused widespread fiber-matrix interfacial sep-

TABLE II
Summary of Flexure Test Results

	Maximum load		Flexural stiffness		
Test specimens	Load (N)	% Change	Modulus (GPa)	Stiffness (N/mm)	% Change
Baseline	6.51 (9.7)*	0	125 (2.6*)	4.06 (2.6)	0
Mil-L-7808 soaked	6.84 (4.1)	+5	125 (1.7)	4.06 (1.7)	0
Mil-L-23699 soaked	6.39 (5.3)	−2	124 (2.7)	4.04 (2.7)	0
Thermal cycled	1.15 (25.4)	−82	91.4 (9.1)	2.97 (9.1)	−27
Mil-L-7808 soaked + TC	0.86 (30.3)	−87	87.7 (6.6)	2.85 (6.6)	−30
Mil-L-23699 soaked + TC	1.55 (16.9)	−76	102 (5.8)	3.30 (5.8)	−19

* Percent coefficient of variation.

aration and matrix shrinkage, in addition to signs of matrix oxidation. The interfacial separation did impact the tensile strength and fracture strain and flexural modulus. Oil soaking did not change the T_g of the composite rods. However, thermal cycling increased the T_g from 408 to 468°C.

The authors acknowledge Matthew Sharpe and John Skujins of CCMR for their assistance and Dr. Zhigang Xu of CAMSS for the help with SEM.

References

1. Holloway, G.; Mehta, J.; Rosado, L.; Doak, D.; Hubley, C.; Askew, J.; Krawiecki, S. AIAA-2006-4751, 2006, 42nd AIAA/ASME/SAE/ASEE Joint Propulsion Conference and Exhibit, July 9–12, 2006, Sacramento, California.
2. Mahieux, C. A.; Lehmann, D.; desLigneris A. Polym Test 2002, 21, 751.
3. Etxeberria, I.; Franco, J. C.; Valea, A.; Llano-Ponte, R.; Mondragon, I. J Reinf Plast Compos 1995, 14, 989.
4. Hillermeier, R. W.; Seferis J. C. J Appl Polym Sci 2000, 77, 556.
5. Chung, K.; Seferis, J. C. Polymer Degrad Stabil 2001, 71, 425.
6. Parvatareddy, H.; Wang, J. Z.; Dillard, D. A.; Ward, T. C. Compos Sci Technol 1995, 53, 399.
7. Hancox, N. L.; Mater Des 1998, 19, 85.
8. Shimokawa, T.; Katon, H.; Hamaguchi, Y.; Sanbongi S.; Mizuno, H. J Compos Mater 2002, 36, 885.
9. Lee, S.; Nam, J.; Ahn, K.; Chung, K.; Seferis, J. J Compos Mater 2001, 35), 433.
10. Lafarie-Frenot, M. C.; Rouquie, S. Compos Sci Technol 2004, 64, 1725.
11. Chung, K.; Seferis, J. C.; Nam, J. D. Compos A 2000, 31, 945.
12. Lafarie-Frenot, M. S.; Rouquie, S.; Ho, N. Q.; Bellenger V. Compos A 2006, 37, 662.
13. Sinmazcelik, T.; Arici, A. A. J Mater Sci 2006, 41, 1233.
14. Cao, J.; Chen, L. Polym Compos 2005, 26, 713.
15. Lee, B. L.; Holl, M. W. Compos A 1996, 27, 1015.
16. Dutta, P. K.; Kalafut, J.; Lord, H. W. ASME 1988, 9, 192.
17. Kern, K. T.; Long E. R.; Long S.; Harries W. L. Polym Prepr AXS 1990, 31, 611.
18. Abali, F.; Shivakumar, K. N.; Hamidi, N.; Sadler, R. Carbon 2003, 41, 893.